Soliton modulation instability in fiber lasers

D. Y. Tang, L. M. Zhao, X. Wu, and H. Zhang
School of Electrical and Electronic Engineering, Nanyang Technological University, Singapore 639798, Singapore
(Received 21 April 2009; published 11 August 2009)

We report experimental evidence of soliton modulation instability in erbium-doped fiber lasers. An alternate type of spectral sideband generation was always experimentally observed on the soliton spectrum of the erbium-doped soliton fiber lasers when energy of the formed solitons reached beyond a certain threshold value. Following this spectral sideband generation, if the pump power of the lasers was further increased, either a new soliton would be formed or the existing solitons would experience dynamical instabilities, such as the period-doubling bifurcations or period-doubling route to chaos. We point out that the mechanism for this soliton spectral sideband generation is the modulation instability of the solitons in the lasers. We further show that, owing to the internal energy balance of a dissipative soliton, modulation instability itself does not destroy the stable soliton evolution in a laser cavity. It is the strong resonant wave coupling between the soliton and dispersive waves that leads to the dynamic instability of the solitons.

DOI: 10.1103/PhysRevA.80.023806 PACS number(s): 42.65.Tg, 42.55.Wd, 42.60.Fc, 42.65.Re

I. INTRODUCTION

The soliton as a stable localized nonlinear wave has been found in a wide range of physical systems in fluid dynamics, plasma physics, and nonlinear optics. Optical solitons formed as a result of the balanced interplay between the anomalous group velocity dispersion (GVD) and self-phase modulation (SPM) have been observed in pulse propagation in single mode fibers (SMFs) as well as in the mode-locked fiber lasers [1,2]. Recently, it was also shown that solitary waves could even be formed in fiber lasers with net positive cavity dispersion, where the solitons are formed as a result of the effective gain bandwidth limitation under strong cavity nonlinearity [3]. However, different from the soliton formation in single mode fibers, where soliton dynamics is described by the nonlinear Schrödinger equation (NLSE), which is essentially a Hamiltonian system, soliton formation in fiber lasers is governed by the Ginzburg-Landau equation (GLE), which takes into account both the interactions between the fiber dispersion and nonlinear optical Kerr effect and between the gain and loss of a laser. Therefore, solitons formed in a fiber laser are dissipative soliton. While the dynamics of solitons formed in the single mode fibers have been extensively investigated previously, dynamics of dissipative solitons is so far less addressed. As dissipation is a nature of all real physical systems, study on the dynamics and features of dissipative solitons is not only of scientific significance but also of practical importance.

A dissipative soliton has obviously more complicated dynamics than a Hamiltonian soliton. In the case of soliton formation in a mode-locked fiber laser, it was shown that depending on the laser parameters and operation conditions, the solitons formed could have very different properties [4]. While in fiber lasers where the balanced interplay between the SPM and fiber GVD is the dominant effect, solitons formed have properties closely resembling those of the Hamiltonian solitons observed in the single mode fibers; in lasers where the gain-loss balance plays the determined role, properties of the formed solitons have different features from those of the Hamiltonian solitons. In lasers where both effects coexist and interact, the laser emission could become very complicated and without any fixed unique characteristics. Nevertheless, we note that even such a laser emission is still governed by the GLE as demonstrated by the numerical simulations [4].

Obviously, to gain a comprehensive understanding on the solitary pulse operation of a fiber laser, the influence of other cavity components, such as the laser output coupler and intracavity polarizer, as well as the laser cavity boundary condition, should also be considered. In the case of weak influence of them, it is well known that the solitary pulse emission of a fiber laser is essentially determined by the GLE as the impact of the influences is just a perturbation on the GLE solutions [5]. However, whether a formed soliton is stable under strong actions and how a dissipative soliton responds to a strong soliton energy modulation imposed by the cavity boundary condition is still an open question. One of the purposes of soliton fiber laser study is to generate stable high peak power ultranarrow optical pulses. Below the material damage threshold, the pulse with the narrowest pulse width and highest peak power formable in a fiber laser is ultimately limited by the soliton stability. Previous studies have shown that periodic soliton perturbations could generate soliton sidebands due to the periodic soliton shaping and the resonant interference between the solitary wave and dispersive waves [6]. Frequently, it was argued that such a soliton sideband generation could cause soliton instability in a laser and limit the further pulse narrowing [7]. Whether this argument is correct, and what is the true mechanism that destabilizes the solitary waves formed in fiber lasers need to be investigated.

Modulation instability (MI) is a well-known phenomenon that destabilizes strong continuous wave (CW) propagation in dispersive media. In optics, Tai *et al.* first reported experimental observation of MI in light propagation in single mode fibers [8]. They found that MI is physically a special case of four-wave mixing where the phase matching condition is self-generated by the nonlinear refractive index change and the anomalous dispersion of the fibers. Soliton propagation in single mode fibers is intrinsically stable against MI. However, it was theoretically shown that if dispersion of a fiber is

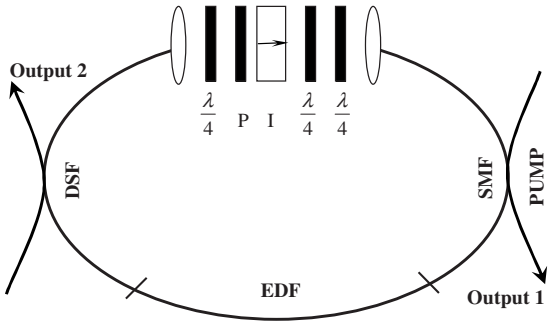

FIG. 1. Schematic of the fiber laser. λ/4: quarter-wave plate; P: polarizer; I: isolator; SMF: single-mode fiber; EDF: erbium-doped fiber; DSF: dispersion-shifted fiber.

periodically varied or the intensity of a solitary wave is periodically modulated, MI could still occur [9,10]. Solitons formed in a fiber laser experience periodic intensity modulation caused by the cavity effect. However, to the best of our knowledge, no soliton modulation instability in lasers has been reported. In this paper we present clear experimental evidence of soliton modulation instability in passively mode-locked fiber lasers. We show experimentally that an alternate type of soliton sideband generation can always be observed on the solitons formed in fiber lasers when energy of the solitons become beyond a certain threshold value. Based on the feature of these sidebands we conclude that they are generated through a parametric coupling process between the solitary waves and the dispersive waves, namely, the modulation instability of the solitons formed in the lasers. MI establishes resonant energy exchange between the solitons and dispersive waves. Nevertheless, it was found that due to the dissipative soliton nature of the laser solitons, the appearance of MI does not destroy the stable evolution of the solitons in a laser. Depending on the concrete laser operation conditions, two consequences of the resonant coupling between the solitons and dispersive waves were experimentally observed. One is the appearance of quasiperiodic soliton intensity modulations, and eventually the soliton shaping of the strong dispersive waves. The other one is the soliton period-doubling bifurcations, and the period-doubling route to chaos. Numerical simulations have well reproduced all the experimental observations. Our research results have shown that MI is an intrinsic feature of the solitons formed in a laser. The development of MI leads to strong resonant wave coupling between the soliton waves and dispersive waves, which further leads to the dynamic instability of a laser soliton. It is the dynamic instability of a soliton that ultimately limits the performance of a soliton laser.

II. EXPERIMENTAL STUDIES AND RESULTS

We conducted experimental studies on soliton fiber lasers with different cavity configurations. Our first experiment was done on a conventional fiber ring laser as shown in Fig. 1. Its cavity was made of three types of SMFs: 3 m erbium-doped fiber (EDF-1480-T6) with GVD of 10 (ps/nm)/km, 2 m dispersion-shifted fiber (DSF) with GVD of 2 (ps/nm)/km, and 12.3 m of the standard SMF. The nonlinear polarization

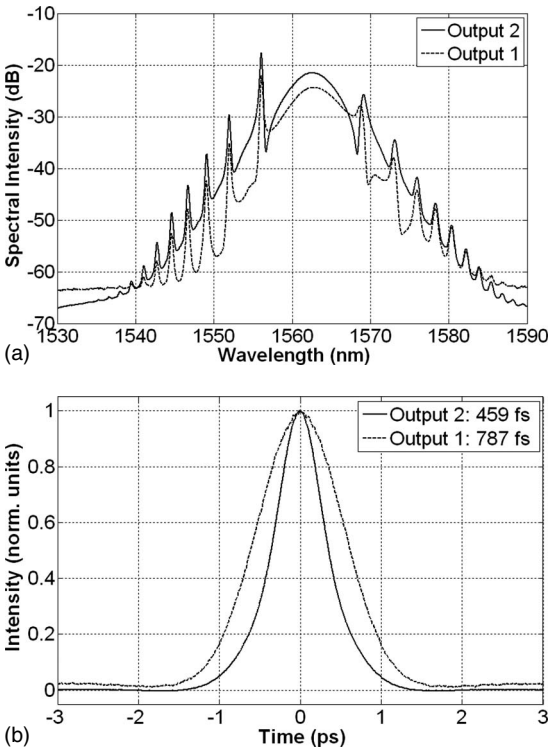

FIG. 2. A typical soliton operation state of the laser at different outputs: (a) Optical spectra; (b) Autocorrelation traces.

rotation technique was used to achieve the self-started mode locking of the laser. To this end a polarizer together with three quarter-wave plates was used to adjust the polarization of light in the cavity. The unidirectional operation of the laser was forced by a polarization independent isolator inserted in the laser cavity. The polarizer, quarter-wave plates, and the isolator were mounted on a 76-mm-long fiber bench. The fiber output coupler is made of the DSF. It has 10% output coupling. Apart from the output from the output coupler (output 2), we also measured the light coupled out of the cavity through the spare pigtail of the wavelength-division-multiplexer (WDM) (output 1) to monitor the pulse evolution in the cavity.

Depending on the orientations of the wave plates and the polarizer, solitons with different parameters could always be obtained. Figure 2 shows for example the optical spectra and autocorrelation traces of a soliton operation of the laser at the above two cavity output ports. Although all the fibers used have anomalous dispersion, it was found that the soliton pulse parameters varied along the cavity. Measured at the output port 1, the pulse had a broad pulse width (787 fs if a sech^2 pulse is assumed) and low pulse energy (189 pJ). The pulse was amplified passing through the gain segment. It then became a narrow (459 fs) and strong (575 pJ) pulse, as measured at the output port 2. We note that there was only one pulse existing in the cavity. Figure 3 shows the change in the soliton optical spectrum with the pump power increase. To clearly show the variations in the spectra, we have artificially offset the spectra by 5 dB with each other. At low pump power, the soliton spectrum is smooth, only the spectral sidebands caused by the resonant interference between

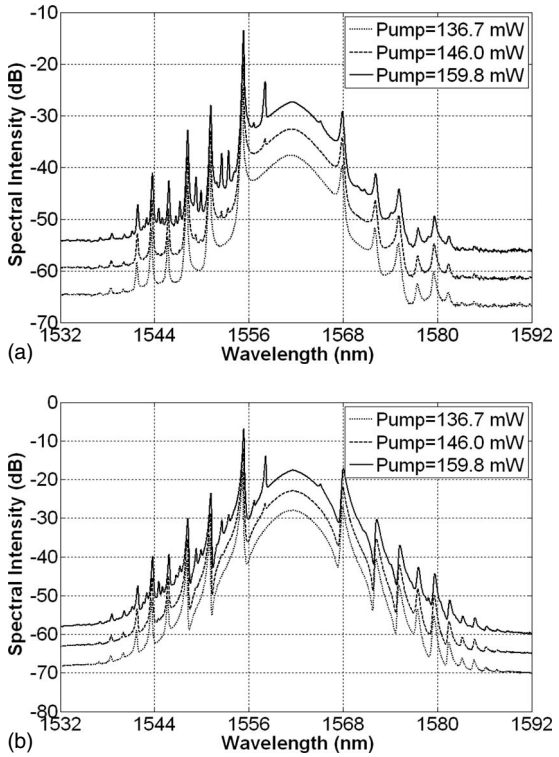

FIG. 3. Experimentally measured soliton spectra under different pump strengths at (a) Output 1; (b) Output 2.

the soliton and dispersive waves are observed. The positions of the spectral sidebands on the soliton spectrum are determined by the cavity dispersion and the soliton pulse width [6]. We will call these spectral sidebands as the resonant sidebands. As the pump strength was increased, a new set of sidebands suddenly emerged on the soliton spectrum, initially obvious on the short-wavelength side of the spectrum. As the pump strength increased to 159.8 mW, the symmetrical counterparts of the newly appearing spectral sidebands on the long-wavelength side of the spectrum also became visible. In addition, a new set of sidebands had also appeared at the pump power strength. The process of this spectral sideband generation was reversible. When the pump power was decreased, the newly formed sidebands could be completely removed from the spectrum. We emphasize the differences between the newly formed spectral sidebands and the resonant sidebands. First, the formation of the resonant sidebands is not a threshold effect. As far as a soliton is formed in fiber lasers, the resonant sidebands are observed, while the newly formed spectral sidebands only appear when the pump power is increased, thereby the soliton intensity is beyond a certain threshold value. Second, the positions of the newly formed sidebands on the soliton spectrum are the pump strength dependent, while those of the resonant sidebands are mainly determined by the cavity dispersion [6]. Under the current laser operation condition the newly formed sidebands are pronounced on the short-wavelength side of the spectrum. This is because the cavity loss of the laser has a sinusoidal form of wavelength dependence [11]. Under the current cavity parameter setting, sidebands on the long-wavelength side of the spectrum experience large cavity loss. Experimentally

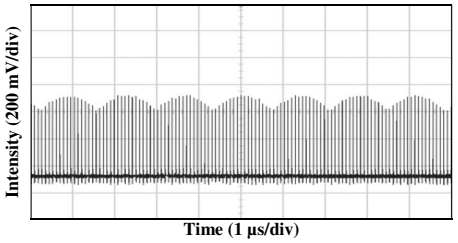

FIG. 4. Experimentally measured oscilloscope trace of the laser soliton emission. Pump power=159.8 mW.

through changing the laser mode locking regime, one can also swap the side of large cavity loss on the soliton spectrum. In our experiments cases where the strong sidebands appeared on the long-wavelength side had also been observed. However, limited by the mode locking feature of the laser, it is experimentally difficult to obtain the case where the new sidebands have exactly the same strength on both sides of the spectrum.

Even after the new spectral sidebands were formed on the soliton spectrum, the soliton operation of the laser initially still remained stable. However, as the spectral strength of the new sidebands increased, the soliton then gradually lost its stability. Depending on the laser operation conditions, two different consequences were experimentally observed. In one case, as the pump power was carefully increased, the soliton energy initially became slowly periodic modulated. A typical case is shown in Fig. 4. The modulation then quickly became quasiperiodic. Eventually a new soliton was formed in the cavity. Associated with the formation of the new soliton, the new sidebands also disappeared. However, the resonant sidebands still remained on the soliton spectrum. The two solitons were stable in the cavity and they had identical pulse parameters. Further increasing the pump power, the same procedure as described above was then repeated. This situation was the most frequently observed case. In another case, as the pump power was increased, instead of the periodic or quasiperiodic soliton energy modulations, the soliton energy experienced a period-doubling bifurcation, characterized as that the energy of the soliton returned to its previous value after every two cavity roundtrips. Occasionally, a higher order of period-doubling bifurcation and even the soliton period-doubling route to chaos were observed. The situation also ends with the formation of a new soliton. Moreover as the pump power was continuously increased, the whole above procedure was repeated.

To check whether the observed new soliton sideband generation is a general property of the laser solitons or it is only related to solitons formed in a specific laser, we further experimentally investigated the soliton feature in other soliton fiber lasers. For this purpose we then removed the DSF, and replaced the negative dispersion erbium-doped fiber with a piece of positive dispersion erbium-doped fiber, whose GVD is about -50 ps/nm/km, and constructed a dispersion-managed cavity (DMC) fiber laser. The same mode locking technique was used for the DMC fiber laser. An advantage of using a DMC is that through changing the length of the SMF, the net cavity dispersion can be easily changed from the negative values to the positive values. Therefore, different

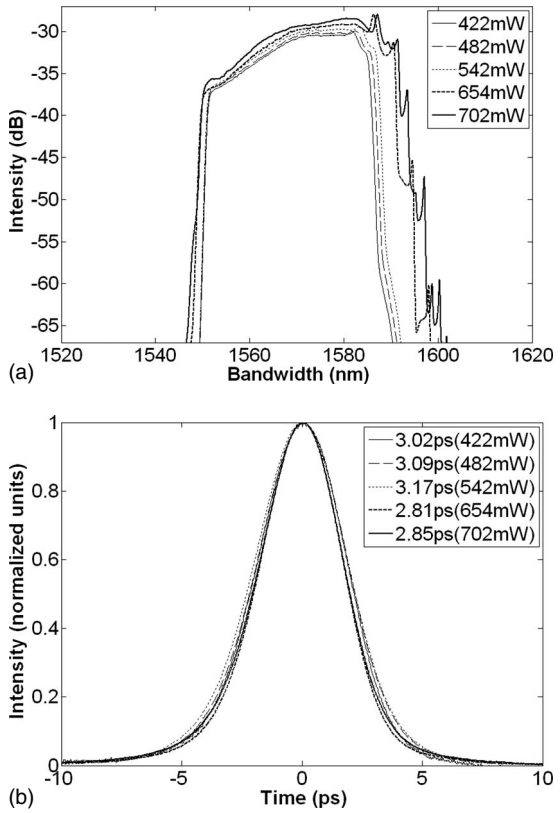

FIG. 5. Experimentally measured GGSs under different pump strengths. (a) Optical spectra; (b) Autocorrelation traces.

types of solitons could be obtained and their dynamics in the laser cavity could be studied. Indeed experimentally when the net cavity GVD was set large negative, the conventional soliton operation of the erbium-doped fiber lasers was observed; near the zero net cavity GVD, either the dispersion-managed (DM) soliton operation [12] or the stretched pulses [13] could be observed, while in the regime of large net positive cavity GVD, the gain-guided solitons (GGSs) were obtained [3]. In two previous papers we have reported the experimental observations of soliton period-doubling bifurcations and period-doubling route to chaos in DM fiber lasers operating in the largely negative or around zero cavity GVD regimes, respectively [14,15]. It was found that under strong soliton intensity, the period of the soliton circulation in cavity could become doubled. Associated with each soliton period-doubling bifurcation, new sets of soliton sidebands appeared on the soliton spectrum, and the new spectral sidebands appeared pairwise with respect to the soliton carrier frequency [16].

Here we will focus on the GGS operation of the DMC fiber laser. Again it was experimentally found that with appropriate selection of the laser operation conditions, the new type of soliton sideband generation could be obtained on the GGSs. Figure 5 shows for example the optical spectra and the corresponding autocorrelation traces of the GGSs under different pump strengths. Different from the solitons formed in the negative cavity GVD regime, where the soliton spectrum shows the characteristic resonant sidebands, the spectrum of the GGSs has initially no spectral sidebands. In contrast, the spectrum of the GGSs is characterized by their steep spectral edges. The soliton spectral difference is traced back to their different soliton formation mechanisms and soliton properties. While the solitons formed in the large negative cavity GVD regime are almost transform-limited pulses, the GGSs are strongly chirped pulses [3]. At low pump power, the GGS spectrum was smooth. As the pump strength was increased, the width of the spectral profile expanded. To the pump strength of 654 mW, spectral sidebands suddenly appeared on the long wavelength edge of the soliton spectrum. Further increasing the pump strength to 702 mw, a new set of spectral sidebands also appeared on the spectrum.

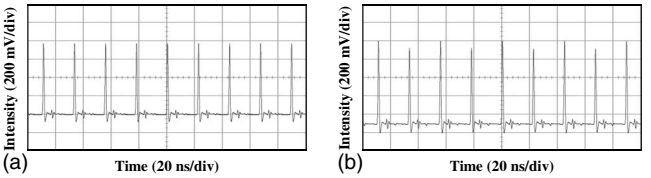

FIG. 6. Experimentally measured oscilloscope traces of the GGSs. (a) Pump=654 mW and (b) Pump=702 mW.

Figure 6(a) shows the oscilloscope trace of the soliton after the spectral sidebands appeared. It was found that the GGSs were still stable. However, when the pump strength was increased to 702 mW, the soliton then experienced a period-doubling bifurcation as shown in Fig. 6(b). Associated with the soliton period-doubling a set of spectral "subsidebands" appeared on the soliton spectrum, which is exactly the same as the period-doubling bifurcation of the solitons in the negative GVD fiber lasers [16]. Limited by the cavity peak power clamping effect, no further period-doubling bifurcation but the noiselike pulses emission of the GGS was observed if the pump strength was continuously increased.

III. NUMERICAL SIMULATIONS

Our experimental results clearly demonstrated that the generation of the new type of soliton sidebands is a general feature of the solitons formed in a laser. Its appearance is independent of the detailed laser cavity configurations as well as the property of the formed solitons. To confirm our experimental observations, we have also numerically simulated the laser soliton feature. For our numerical simulations we used exactly the same model as reported in [17]. With the model we had previously numerically reproduced the soliton period-doubling route to chaos in fiber lasers with net negative and near zero cavity dispersion [16]. Briefly, we used the following coupled extended Ginzburg-Landau equations to describe the soliton propagation in the cavity fibers:

$$\frac{\partial u}{\partial z} = -i\beta u + \delta\frac{\partial u}{\partial t} - \frac{ik''}{2}\frac{\partial^2 u}{\partial t^2} + \frac{ik'''}{6}\frac{\partial^3 u}{\partial t^3} + i\gamma\left(|u|^2 + \frac{2}{3}|v|^2\right)u + \frac{i\gamma}{3}v^2u^* + \frac{G}{2}u + \frac{G}{2\Omega_g^2}\frac{\partial^2 u}{\partial t^2}$$

$$\frac{\partial v}{\partial z} = i\beta v - \delta\frac{\partial v}{\partial t} - \frac{ik''}{2}\frac{\partial^2 v}{\partial t^2} + \frac{ik'''}{6}\frac{\partial^3 v}{\partial t^3} + i\gamma\left(|v|^2 + \frac{2}{3}|u|^2\right)v + \frac{i\gamma}{3}u^2 v^* + \frac{G}{2}v + \frac{G}{2\Omega_g^2}\frac{\partial^2 v}{\partial t^2} \quad (1)$$

where u and v are the normalized envelopes of the pulses along the two orthogonal polarization axes of the fiber. $2\beta = 2\pi\Delta n/\lambda$ is the wave-number difference between the two modes. $2\delta = 2\beta\lambda/2\pi c$ is the inverse group velocity difference. k'' is the second-order dispersion coefficient, k''' is the third-order dispersion coefficient, and γ represents the nonlinearity of the fiber. G is the saturable gain of the fiber. For the undoped fiber $G=0$, and for the erbium-doped fiber we further considered the gain saturation as

$$G = G_0 \exp\left[-\frac{\int(|u|^2 + |v|^2)dt}{E_{\text{sat}}}\right], \quad (2)$$

where G_0 is the small signal gain coefficient and E_{sat} is the normalized saturation energy.

Following the soliton circulation in the cavity, we took into account the actions of each cavity components by multiplying their Jones matrix to the soliton field when the soliton met them. With the technique we automatically included the effects of the periodical soliton energy and cavity dispersion variations on the soliton. For the case of all-negative dispersion fiber laser, we used the following parameters for possibly matching them to our experimental conditions: nonlinear fiber coefficient $\gamma=3\ \text{W}^{-1}\,\text{km}^{-1}$, central wavelength of 1560 nm, fiber dispersions $k''_{\text{EDF}}=-12.8\ \text{ps}^2/\text{km}$, $k''_{\text{SMF}}=-23.0\ \text{ps}^2/\text{km}$, $k''_{\text{DSF}}=-2.6\ \text{ps}^2/\text{km}$, and $k'''=-0.13\ \text{ps}^3/\text{km}$, beat length $L_b=\text{L}/2$, $\Omega_g=16$ nm, cavity length $L=13_{\text{SMF}}+3_{\text{EDF}}+1.0_{\text{DSF}}+10\%\ \text{Output}+1.0_{\text{DSF}}=18$ m, the orientation of the intracavity polarizer to the fiber fast birefringent axis $\Psi=0.152\pi$, and gain saturation energy $E_{\text{sat}}=300$ pJ. The linear cavity phase delay bias was set to $\text{Ph}=1.5\pi$ in the simulation.

Numerically we could well reproduce the new type of sideband generation, as shown in Fig. 7. Under a weak pump strength of $G_0=670\ \text{km}^{-1}$, the optical spectrum is smooth and has only the characteristic resonant sidebands. When the pump strength is increased to $G_0=770\ \text{km}^{-1}$, apart from the resonant sidebands, new spectral sidebands appeared on the short wavelength side of the spectrum, which qualitatively agrees with the experimental observation. Figure 8 shows the numerically simulated pulse train corresponding to Fig. 7(b), the quasiperiodic pulse intensity fluctuation is similar to the experimental observations. We note that even the numerically calculated spectral sidebands are asymmetric with respect to the soliton central wavelength. It is well known that the third-order dispersion could also lead to asymmetric spectral sidebands on the soliton spectrum [18]. To confirm that the calculated spectral sidebands were not caused by the third-order material dispersion effect, we deliberately removed the third-order dispersion terms from the coupled GLEs. Without third-order dispersion, almost the same results as shown in Fig. 8 were obtained, which indicated that the third-order dispersion did not play a big role on the formation of the observed sidebands. This result should be understandable. As the second-order dispersion of the fibers used is over one order of magnitude larger than the third-order dispersion, effects caused by the third-dispersion is ignorable. We point out that the wavelength-dependent cavity loss effect of the laser is included in our numerical simulations [17]. Intrinsic to the nonlinear polarization mode locking technique used, the effective cavity transmission is in fact a wavelength dependent function with a sine-squared form. Depending on the orientation of the intracavity polarizer with respect to the fiber fast birefringent axis, mode locking can only be established in the wavelength range along one edge of the cavity transmission curve, which results in that the effective gain of the laser is always asymmetric with respect to the soliton central wavelength.

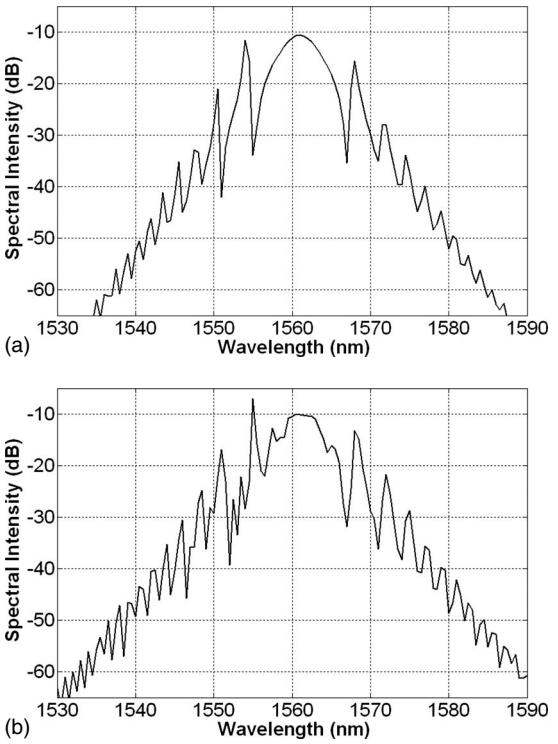

FIG. 7. Numerically calculated optical spectra of the soliton under different pump strengths. (a) $G_0=670\ \text{km}^{-1}$ and (b) $G_0=770\ \text{km}^{-1}$.

For the DMC fiber laser, we used the following parameters for the simulations: nonlinear fiber coefficient $\gamma=3\ \text{W}^{-1}\,\text{km}^{-1}$, central wavelength of 1570 nm, fiber disper-

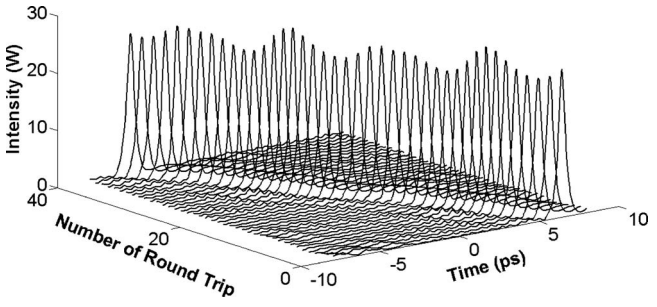

FIG. 8. Numerically calculated soliton evolution with the cavity roundtrips at $G_0=770\ \text{km}^{-1}$.

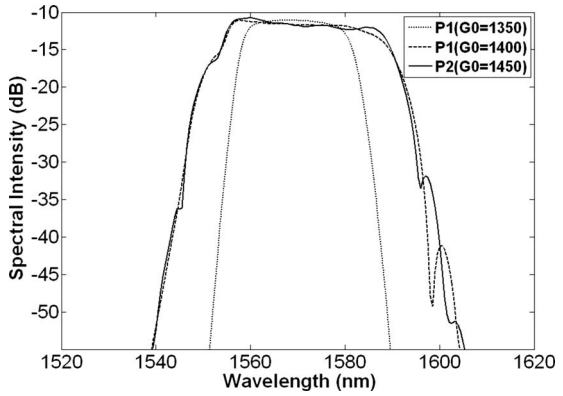

FIG. 9. Numerically calculated optical spectra of the GGSs under different pump strengths.

sions $k''_{\mathrm{EDF}}=41.85\ \mathrm{ps}^2/\mathrm{km}$, $k''_{\mathrm{SMF}}=-23.54\ \mathrm{ps}^2/\mathrm{km}$, and $k'''=-0.13\ \mathrm{ps}^3/\mathrm{km}$, beat length $L_b=\mathrm{L}/2$, $\Omega_g=16$ nm, cavity length $L=0.8_{\mathrm{SMF}}+2.7_{\mathrm{EDF}}+0.3_{\mathrm{SMF}}+10\%$ Output$+0.7_{\mathrm{SMF}}=4.5$ m, the orientation of the intracavity polarizer to the fiber fast birefringent axis $\Psi=0.152\pi$, and gain saturation energy $P_{\mathrm{sat}}=1000$ pJ. The linear cavity phase delay bias was set to $\mathrm{Ph}=1.85\pi$ in the simulation. Again, we could numerically reproduce the alternate type of soliton sideband generation and the period-doubling bifurcation of the GGSs. Figures 9 and 10 show the results of numerical simulations. Under weak pump strength, the GGS spectrum is smooth and has the characteristic steep spectral edges. When the pump strength is increased to $G_0=1400\ \mathrm{km}^{-1}$, spectral sidebands appeared on the long wavelength edge of the spectrum. However, the appearance of the spectral sidebands did not affect the soliton stability as evidenced by Fig. 10(a). Further increasing pump strength to $G_0=1450\ \mathrm{km}^{-1}$, the soliton then

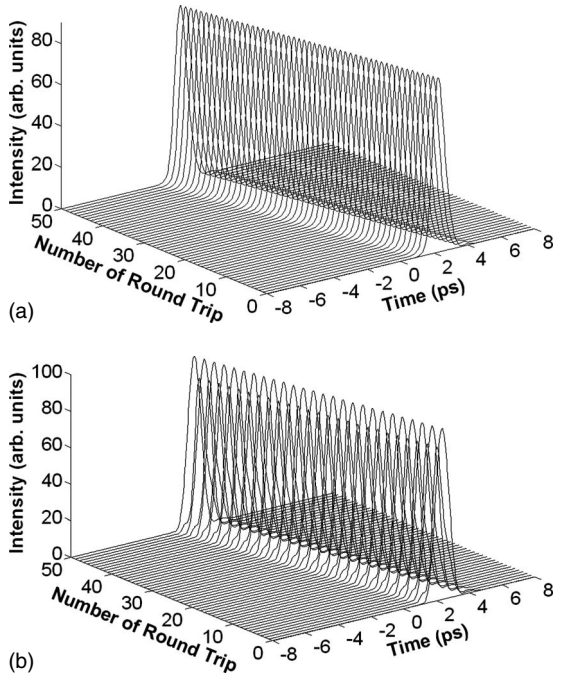

FIG. 10. Numerically calculated soliton evolution with the cavity roundtrips. (a) $G_0=1400\ \mathrm{km}^{-1}$ and (b) $G_0=1450\ \mathrm{km}^{-1}$.

experienced a period-doubling bifurcation [Fig. 10(b)]. Associated with the soliton period-doubling bifurcation, extra spectral sidebands appeared on the soliton spectrum as shown in Fig. 9. Like the experimental observations, the sidebands appeared only on the spectral edges, and their positions shifted with the pump strength.

IV. DISCUSSIONS

Obviously there are two types of soliton sideband generation in a soliton fiber laser. One is the resonant sidebands generation. The formation mechanism of the resonant sidebands has been extensively investigated previously [6,7]. The resonant sideband generation is a linear effect. Another one is the reported new type of soliton sideband generation. It is a threshold effect and only appears when the solitons formed in a laser have sufficiently strong energy. The symmetrical appearance of the sidebands with respect to the central soliton spectral wavelength together with the threshold feature of the sideband generation suggests that the new sidebands were generated through a parametric process between the soliton and the dispersive waves, namely, it is a result of the soliton modulation instability. It is a well-known fact that the optical solitons formed in SMFs are intrinsically stable against MI. However, our experimental results as well as the numerical simulations have clearly demonstrated that MI of a laser soliton is possible. To understand why a laser soliton could exhibit MI, we note that Matera *et al.* theoretically showed that periodic soliton energy modulation could induce parametric spectral sideband generation [9]. We found that the observed new type of soliton spectral sideband generation could be well explained based on the theoretical prediction. Due to the cavity output coupling, laser gain amplification, and the laser cavity boundary condition, a soliton circulating in the laser cavity has intrinsic periodic energy variation. Therefore, it is to expect that under strong periodic soliton energy variation the above-predicted soliton MI could occur on the formed laser soliton. However, it is to further note that because the soliton is now circulating in the laser cavity, the cavity resonance condition also plays a role, as have been theoretically predicted by Coen *et al.* [19], the MI sideband positions are no longer purely determined by the cavity length, but also vary with the cavity detuning.

Soliton MI causes resonant energy coupling between soliton and dispersive waves. As observed experimentally, a soliton could still maintain stable circulation in the cavity after MI. This is because the laser solitons are dissipative soliton; their internal energy balance can adapt the soliton energy loss. However, as the resonant energy coupling between the soliton and dispersive waves becomes strong, the strong resonant interaction between the waves could then drive the soliton into a dynamic instability. The latter effect is in fact a generic feature of all nonlinear dynamic systems [20–22]. Numerically we found whether a soliton experiences the quasiperiodic bifurcations and route to chaos or the period-doubling bifurcations and route to chaos depends on where the MI sidebands are formed on the soliton spectrum, which is in turn related to the linear cavity phase detuning. Certainly in a net negative dispersion fiber laser when the dis-

persive waves become too strong, they could also be shaped into a soliton, while in a net positive dispersion fiber laser this would be much more difficult. Based on our study it also becomes clear that the ultimate limitation on the narrowest pulse formation in a mode-locked laser is neither the resonant soliton sideband generation nor the soliton MI, but the dynamic instability of the soliton. A recent experimental result on the ultrashort pulse formation in a Ti:Sapphire solid-state laser seemed also implicitly support the point [23].

V. CONCLUSIONS

In conclusion, we have demonstrated experimental evidence of soliton modulation instability in erbium-doped fiber lasers. We have shown that as a result of the periodic soliton energy variation in the laser cavity, parametric coupling between the soliton pulse and the dispersive waves could be established, which results in a threshold type of spectral sideband formation. Nevertheless, even under existence of soliton modulation instability a dissipative soliton could be still stable, as its internal energy balance can adapt the energy coupling. However, under strong coupling between the soliton and dispersive waves, the nonlinear wave mixing can drive the soliton into dynamic instability. It is the dynamic instability of a soliton in a laser that ultimately limits the narrowest and highest peak power pulse formation in a mode locked laser.

[1] L. F. Mollenauer, R. H. Stolen, and J. P. Gordon, Phys. Rev. Lett. **45**, 1095 (1980).
[2] V. J. Matsas, T. P. Newson, D. J. Richardson, and D. N. Payne, Electron. Lett. **28**, 1391 (1992).
[3] L. M. Zhao, D. Y. Tang, and J. Wu, Opt. Lett. **31**, 1788 (2006).
[4] D. Y. Tang, L. M. Zhao, G. Q. Xie, and L. J. Qian, Phys. Rev. A **75**, 063810 (2007).
[5] H. A. Haus, J. G. Fujimoto, and E. P. Ippen, IEEE J. Quantum Electron. **28**, 2086 (1992).
[6] S. M. J. Kelly, Electron. Lett. **28**, 806 (1992).
[7] M. L. Dennis and I. N. Duling III, Appl. Phys. Lett. **62**, 2911 (1993).
[8] K. Tai, A. Hasegawa, and A. Tomita, Phys. Rev. Lett. **56**, 135 (1986).
[9] F. Matera, A. Mecozzi, M. Romagnoli, and M. Settembre, Opt. Lett. **18**, 1499 (1993).
[10] N. J. Smith and N. J. Doran, Opt. Lett. **21**, 570 (1996).
[11] W. S. Man, H. Y. Tam, M. S. Demokan, P. K. A. Wai, and D. Y. Tang, J. Opt. Soc. Am. B **17**, 28 (2000).
[12] Y. Kodama, S. Kumar, and A. Maruta, Opt. Lett. **22**, 1689 (1997).
[13] K. Tamura, E. P. Ippen, H. A. Haus, and L. E. Nelson, Opt. Lett. **18**, 1080 (1993).
[14] L. M. Zhao, D. Y. Tang, F. Lin, and B. Zhao, Opt. Express **12**, 4573 (2004).
[15] L. M. Zhao, D. Y. Tang, T. H. Cheng, H. Y. Tam, C. Lu, and S. C. Wen, Opt. Commun. **278**, 428 (2007).
[16] D. Y. Tang, J. Wu, L. M. Zhao, and L. J. Qian, Opt. Commun. **275**, 213 (2007).
[17] D. Y. Tang, L. M. Zhao, B. Zhao, and A. Q. Liu, Phys. Rev. A **72**, 043816 (2005).
[18] M. Santagiustina, J. Opt. Soc. Am. B **14**, 1484 (1997).
[19] S. Coen and M. Haelterman, Phys. Rev. Lett. **79**, 4139 (1997).
[20] Y. Silberberg and I. Bar Joseph, Phys. Rev. Lett. **48**, 1541 (1982).
[21] I. Bar-Joseph and Y. Silberberg, Opt. Commun. **48**, 53 (1983).
[22] H. Nakatsuka, S. Asaka, H. Itoh, K. Ikeda, and M. Matsuoka, Phys. Rev. Lett. **50**, 109 (1983).
[23] A. Fernandez, T. Fuji, A. Poppe, A. Fürbach, F. Krausz, and A. Apolonski, Opt. Lett. **29**, 1366 (2004).